Letter

Integration of a Hydrogenase in a Lead Halide Perovskite Photoelectrode for Tandem Solar Water Splitting

Esther Edwardes Moore, Virgil Andrei, Sonia Zacarias, Inês Antunes Cardoso Pereira, and Erwin Reisner

Just Accepted

Integration of a Hydrogenase in a Lead Halide Perovskite Photoelectrode for Tandem Solar Water Splitting

Esther Edwardes Moore[†], Virgil Andrei[†], Sónia Zacarias[‡], Inês A. C. Pereira[‡], Erwin Reisner[†*]

[†]Department of Chemistry, University of Cambridge, Lensfield Road, Cambridge CB2 1EW, U.K.

[‡]Instituto de Tecnologia Química e Biológica António Xavier, Universidade Nova de Lisboa, Av. da Republica, 2780-157 Oeiras, Portugal

Supplementary information placeholder

ABSTRACT: Perovskite solar cells are notoriously moisture-sensitive, but recent encapsulation strategies have demonstrated their potential application as photoelectrodes in aqueous solution. However, perovskite photoelectrodes rely on precious metal co-catalysts and their combination with biological materials remains elusive. Here, we interface [NiFeSe] hydrogenase from *Desulfovibrio vulgaris* Hildenborough, a highly active enzyme for H_2 generation, with a triple cation mixed halide perovskite. The perovskite-hydrogenase photoelectrode produces a photocurrent of -5 mA cm^{-2} at 0 V *vs.* RHE during AM1.5G irradiation, is stable for 12 h and the hydrogenase exhibits a turnover number of $1.9 \cdot 10^6$. The positive onset potential of $+0.8$ V *vs.* RHE allows its combination with a $BiVO_4$ water oxidation photoanode to give a self-sustaining, bias-free photoelectrochemical tandem system for overall water splitting (solar-to-hydrogen efficiency of 1.1%). This work demonstrates the compatibility of perovskite elements with biological catalysts to produce hybrid photoelectrodes with benchmark performance, which establishes their utility in semi-artificial photosynthesis.

As a globally abundant and economical energy source, solar energy is the fastest growing renewable alternative to fossil fuels.[1, 2] Artificial photosynthesis uses sunlight for the production of renewable chemical fuels, so-called solar fuels, thus addressing the intermittency limitations of photovoltaic (PV) technologies.[3, 4] Solar fuel synthesis can be achieved by direct coupling of an efficient light absorber to a fuel-producing catalyst.[5, 6] Organic-inorganic lead halide perovskites have received much attention due to their low production costs and promising PV cell efficiencies, currently reaching up to 25.2%.[2, 7-10] However, moisture, air and temperature instability has challenged the use of perovskites in photoelectrochemical (PEC) devices.[11, 12] Encapsulation layers such as eutectic metal alloys, metal foils and epoxy resin have improved the operation lifetime of solution immersed perovskite-based photoelectrodes from seconds to hours.[11, 13-17] However, all H_2-evolving PEC perovskite photocathodes have employed high cost, low abundance Pt nanoparticles as the co-catalyst to date.

Semi-artificial photosynthesis combines the evolutionarily-optimized activity of biological catalysts such as isolated enzymes with synthetic photoabsorbers.[18-21] Hydrogenases (H_2ases) are reversible and highly efficient H_2 production enzymes with a per active-site activity matching Pt.[22-24] The integration of H_2ase with Si and Cu_2O photocathodes has previously been achieved,[25-29] but the combination with a perovskite has remained inaccessible due to the moisture sensitivity of this photoabsorber and difficulty of achieving a productive enzyme-photoabsorber interface.

Here, a perovskite-H_2ase photocathode is presented, realized by an encapsulation system that protects the photoabsorber and provides a biocompatible, bespoke porous scaffold for the enzyme. This semi-artificial photocathode enabled combination with a $BiVO_4$ water oxidation photoanode for bias-free, tandem PEC water splitting into H_2 and O_2 (Figure 1).
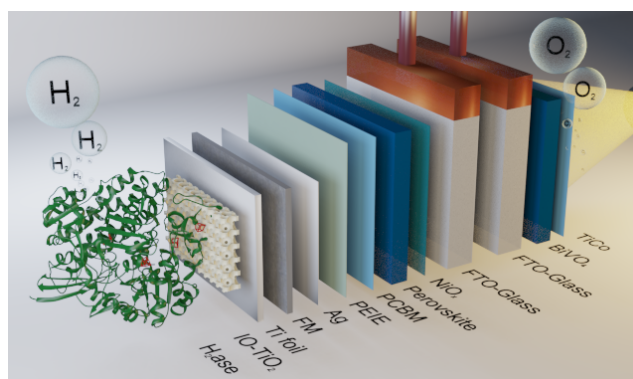
Figure 1. Schematic representation of the tandem PEC cell consisting of a FM-encapsulated perovskite photocathode with H_2ase integrated into an IO-TiO_2 layer and a $BiVO_4$ photoanode. TiCo refers to the water oxidation layer precursor: $[Ti_4O(OEt)_{15}(CoCl)]$. PCBM: [6,6]-phenyl C_{61} butyric acid methyl ester. PEIE: polyethylenimine.

Optimized cesium formamidinium methylammonium (CsFAMA) triple cation mixed halide perovskite devices with a Field's metal (FM) protection layer were assembled and characterized as previously reported (Figure 1; see SI Experimental Procedures and Figure S1 for details).[15] Enzymes have been integrated with high loading into hierarchically structured, macro and mesoporous, inverse opal (IO) metal oxide scaffolds.[25, 30, 31] TiO_2, an established enzyme interface, was selected for its stability and conductivity under reducing conditions.[25, 32, 33] The high-temperature (>100 °C) sensitivity of the perovskite prevented *in situ* annealing of the IO-TiO_2 directly on the FM surface. Therefore, anatase TiO_2 nanoparticles (~21 nm Ø) were first co-assembled with polystyrene beads

(750 nm Ø) on Ti foil and annealed at 500 °C to give Ti|IO-TiO$_2$ (Figure S2). The geometrical surface area of the IO-TiO$_2$ scaffold was 0.28 cm^2 with an IO-TiO$_2$ film thickness of 15 μm. The Ti|IO-TiO$_2$ was then joined to the protected perovskite by briefly melting the FM sheet *via* a Peltier thermoelectric element (at ~70 °C) and an epoxy resin was used to seal the edges to give the encapsulated photovoltaic-integrated photocathode: PVK|IO-TiO$_2$

[FTO-glass|NiO$_x$|perovskite|PCBM|PEIE|Ag|FM|Ti|IO-TiO$_2$].

A [NiFeSe] H$_2$ase from *Desulfovibrio vulgaris* Hildenborough (*Dv*H) was selected due to its considerable H$_2$ evolution activity compared to *Dv*H [NiFe] H$_2$ase, and purified and characterized as previously reported.[23, 33-37] The selenocysteine residue (Sec489) in the active site (Figure S3) causes improved O$_2$ tolerance,[35, 37-40] which is beneficial for its application in overall water splitting. The [NiFeSe] H$_2$ase (5 μL, 50 pmol) was dropcast onto Ti|IO-TiO$_2$ and left to saturate the film for 30 min in a N$_2$ atmosphere. Protein film voltammetry of the Ti|IO-TiO$_2$|H$_2$ase electrode in a three-electrode configuration demonstrated that proton reduction occurred with minimal overpotential, indicative of efficient charge transfer at the TiO$_2$-hydrogenase interface (Figure S4). The quality of the interface can be attributed to the well-known strength of protein binding to TiO$_2$, an effect which may be further accentuated by polarisation of the TiO$_2$ surface.[25, 33, 41] The Ti|IO-TiO$_2$|H$_2$ase electrode displayed current densities of −2.5 mA cm^{-2} with high stability for several hours at an applied potential (E$_{app}$) of −0.5 V *vs.* RHE under N$_2$, including some robustness in the presence of O$_2$. A Faradaic efficiency for H$_2$, FE$_{H_2}$, after 24 h of 78% was determined by gas chromatography. The E$_{app}$ of −0.5 V *vs.* RHE was applied to reflect the estimated perovskite photovoltage of 0.9 V in the PEC experiments, where an E$_{app}$ of +0.4 V *vs.* RHE has been applied (see below).

Protein-film photoelectrochemistry of the PVK|IO-TiO$_2$|H$_2$ase photocathode (three-electrode configuration, H$_2$ase integrated as above) was conducted at 25 °C under chopped simulated solar light irradiation (100 mW cm^{-2}, AM1.5G). The photocathode was irradiated from the back, which prevented photoexcitation of TiO$_2$. Linear sweep voltammetry (LSV) of the assembled PVK|IO-TiO$_2$|H$_2$ase electrode showed a cathodic onset potential at +0.8 V *vs.* RHE and photocurrent densities of −5 mA cm^{-2} at 0 V *vs.* RHE (Figure 2a).

Controlled potential photoelectrolysis (CPPE) was conducted at +0.4 V *vs.* RHE and gas chromatography used to quantify H$_2$ evolution yields. CPPE demonstrated the stability of the photocathode, which consistently achieved 12 h of catalysis (Figure 2b). Failure of the enzyme-photocathode after 12 h was likely due to water influx into the encapsulated perovskite, consistent with previous reports (see Figure S5).[13, 15] The stability of the equivalent PVK-Pt device was found to be comparable, supporting failure of the perovskite as the limit to longevity (Figure S6). The H$_2$ase electrode generated 258 ± 55 μmol cm^{-2} of H$_2$, whereas the enzyme-free electrode produced <1 μmol$_{H_2}$ cm^{-2} (Figure 2c). The FE$_{H_2}$ of PVK|IO-TiO$_2$|H$_2$ase after 14 h was (91 ± 1.5)% with a H$_2$ase-based turnover number (TON$_{H_2}$) of 1.9·10^6 and turnover frequency (TOF$_{H_2}$) of 95 s^{-1}.
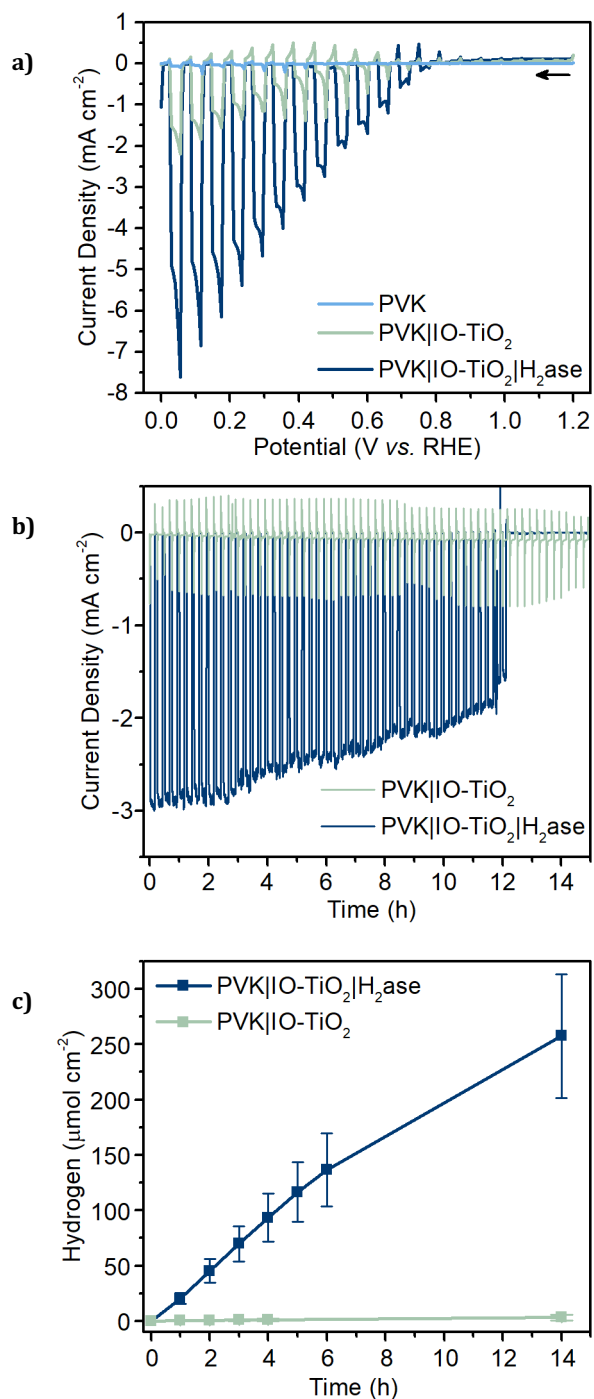
Figure 2. Photoelectrochemistry of biohybrid photocathode. a) Representative LSV of PVK|IO-TiO$_2$|H$_2$ase (blue), PVK|IO-TiO$_2$ (green), PVK (light blue) electrodes with chopped illumination at a scan rate of 10 mV s^{-1}. b) Representative CPPE at E$_{app}$ = +0.4 V *vs.* RHE with a dark period lasting 5 min following every 10 min of light exposure. c) Mean (N = 3) H$_2$ evolution from CPPE quantified by gas chromatography. Conditions: MES (50 mM, pH 6.0), KCl (50 mM), *Dv*H [NiFeSe] H$_2$ase (50 pmol), simulated solar light back-irradiation (AM1.5G, 100 mW cm^{-2}), N$_2$ atmosphere, 25 °C.
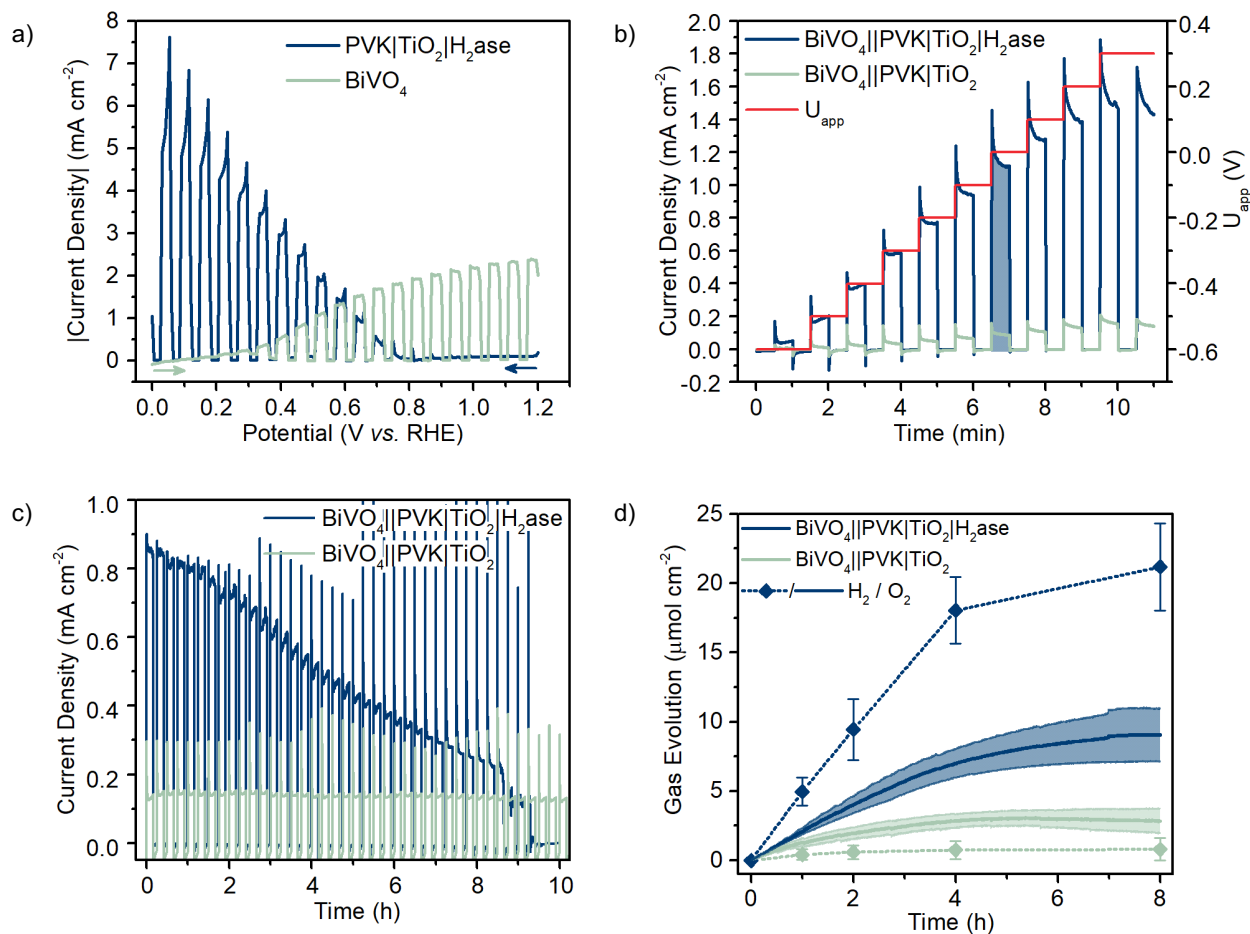
Figure 3. Photoelectrochemistry of the tandem device. a) Representative LSV of PVK|TiO$_2$|H$_2$ase (blue) and BiVO$_4$ (green) electrodes with chopped illumination, forward scan, 10 mV s^{-1} scan rate, showing the absolute current densities. b) Representative Stepped potential chronoamperometry of BiVO$_4$||PVK|TiO$_2$|H$_2$ase (blue) and H$_2$ase-free BiVO$_4$||PVK|TiO$_2$ (green) tandem cells from U_{app} = −0.6 V to +0.3 V. The current density at U_{app} = 0.0 V has been highlighted. c) Representative CPPE of BiVO$_4$||PVK|TiO$_2$|H$_2$ase (blue) and H$_2$ase-free BiVO$_4$||PVK|TiO$_2$ (green) tandem cells at U_{app} = 0.0 V with a dark period lasting 5 min following every 10 min of light exposure. d) Mean (N = 3) H$_2$ (dotted line with measurement points) and O$_2$ (solid line) evolution from CPPE repeats. Conditions: MES (50 mM, pH 6.0), KCl (50 mM), DvH [NiFeSe] H$_2$ase (50 pmol), simulated solar light irradiation (AM1.5G, 100 mW cm^{-2}), N$_2$ atmosphere, 25 °C.

Bias-free tandem water splitting has long been a desirable goal for PEC cells.[25, 31, 42, 43] Here a BiVO$_4$-based water oxidation photoanode was prepared by electrodeposition of BiOI, then dropcasting and annealing a vanadium precursor and finally spin-coating a layer of a cobalt-containing co-catalyst as previously reported.[15, 44] PEC analysis of the photoanode (three-electrode set-up; Figure S7) gave an onset potential of +0.1 V vs. RHE and a current density of 2.4 mA cm^{-2} at +1.23 V vs. RHE.

The positive onset potential of the PVK|IO-TiO$_2$|H$_2$ase photocathode is essential for combination with the BiVO$_4$ photoanode to assemble a tandem water splitting PEC device. The BiVO$_4$ photoanode has been shown to absorb wavelengths below 500 nm and therefore limits the perovskite to absorption at 500-800 nm.[15] Nevertheless, the BiVO$_4$ photoanode remains the current-limiting absorber (Figure 3a). The robustness of the [NiFeSe] H$_2$ase toward O$_2$ (Figure S4) provided the possibility to assemble a 'semi-artificial leaf', where the photoelectrodes were not separated into two compartments by a membrane. The BiVO$_4$||PVK|TiO$_2$|H$_2$ase tandem cell (Figure 1) was

prepared and PEC analysis undertaken in a single compartment cell with illumination through the front of the BiVO$_4$ photoanode.

The two-electrode device achieved a current density of 1.1 mA cm^{-2} under bias-free conditions (U_{app} = 0.0 V) and stepped potential chronoamperometry revealed an onset potential of −0.6 V (Figure 3b). Bias-free CPPE showed a gradual decrease in photocurrent over 8 h, which was attributed to slowly progressing film loss, due to enzyme inactivation, reorientation or desorption (Figure 3c). In agreement, the current density returned to almost the initial value when a sacrificial electron acceptor (methyl viologen) was added to the tandem PEC cell after prolonged irradiation (Figure S8). The peak FE of the device was (82 ± 3)% for H$_2$ and (50 ± 8)% for O$_2$ (Figure 3d, FE over time; Figure S9). The lower FE for O$_2$ can be attributed to some O$_2$ reduction at the photocathode leading to lower amounts of O$_2$ detected. The solar-to-hydrogen efficiency (STH) was 1.1% (Equation S1).

The BiVO$_4$||PVK|TiO$_2$|H$_2$ase cell produced 21.2 ± 3.2 μmol$_{H_2}$ cm^{-2} and 9.0 ± 2.7 μmol$_{O_2}$ cm^{-2} after 8 h

CPPE, giving a H_2:O_2 ratio of 2.3. The PVK|IO-TiO$_2$|H$_2$ase photocathode (Figure S10) and BiVO$_4$||PVK|TiO$_2$|H$_2$ase tandem device (Table 1, Figure S11) compare favourably with state-of-the-art H_2 production PEC systems employing earth abundant molecular catalysts (synthetic and biological) in pH benign aqueous solution (see Tables S1 and S2 for details). Three semi-artificial H_2 evolution photocathodes have been previously reported (Figure S10, colored): a [NiFeSe] H$_2$ase from *Desulfomicrobium baculatum* was introduced onto a p-silicon (p-Si) photoabsorber *via* an IO-TiO$_2$ scaffold,[25] whereas [FeFe] H$_2$ases have been combined with both p-type CuO_2 and black-Si photoabsorbers.[26, 27] Of the systems which employed small molecule catalysts (Figure S10, grey-scale), a Ni Dubois-type catalyst applied to a p-Si photoabsorber, and an Fe-porphyrin and polymeric Co-based catalysts combined with a GaP photocathode provide state-of-the-art performances.[28, 45, 46] Previously reported tandem earth-abundant molecular catalysed PEC water-splitting devices have utilized dye-sensitized p-type semiconductors with cobaloxime H_2 catalysts resulting in STH values below 0.05% (Table 1).[42] A semi-artificial tandem cell with a hydrogenase cathode was wired to an organic dye- photosystem II photoanode, with a STH of 0.14% at 0.3 V applied bias.[31, 47] However, the only previously reported hydrogenase photocathode in a tandem cell employed a p-Si photoabsorber and achieved a STH of 0.006% for bias-free water splitting.[25] The unassisted solar-to-fuel conversion of the BiVO$_4$||PVK|TiO$_2$|H$_2$ase tandem device was also more efficient than previous bacterial bio-hybrid systems.[48] The PVK-H$_2$ase system presented here showed a superior performance to equivalent earth-abundant molecular artificial and biological catalyst systems reported to date.

Table 1. Solar-to-fuel efficiencies of state-of-the-art tandem devices that employ immobilised earth abundant molecular H_2 catalysts, a bacterial catalyst and an analogous Pt device.

System	Tandem cell	Solar-to-fuel / %	Product	ref
Platinum	BiVO$_4$ || PVK|Pt	0.35	H$_2$	[15]
Synthetic	Ru|OD|TiO$_2$ || NiO|OD|Co	0.05	H$_2$	[42]
	TaON|CoO$_x$ || CuGaO$_2$| OD|Co	0.0054	H$_2$	[47]
Enzymatic	IO-TiO$_2$|OD|P$_{0s}$-PSII || IO-ITO|H$_2$ase	0.14 (0.3 V bias)	H$_2$	[31]
	BiVO$_4$ || p-Si|IO-TiO$_2$|H$_2$ase	0.006	H$_2$	[25]
	BiVO$_4$ || PVK|IO-TiO$_2$|H$_2$ase	1.1	H$_2$	This work
Bacterial	TiO$_2$ || Si|TiO$_2$|*S. Ovata*	0.38	Acetate	[48]

OD = organic dye. See Table S2 for details.

In conclusion, the combination of a biocatalyst with a moisture sensitive perovskite photoabsorber has been accomplished and this bio-material hybrid has subsequently been employed in overall tandem solar water splitting. The perovskite-H$_2$ase photocathode was realized by (i) encapsulating the perovskite using a eutectic alloy, metal foil and epoxy resin, and (ii) integrating the enzyme into a hierarchical IO-TiO$_2$ scaffold. The PVK|IO-TiO$_2$|H$_2$ase system achieved benchmark performance for photocathodes driven by earth abundant catalysts with a current density of -5 mA cm^{-2} at 0.0 V *vs*. RHE, a positive onset of $+0.8$ V *vs*. RHE, a H_2 production yield of 258 ± 55 μmol_{H_2} cm^{-2} and a H$_2$ase-based TON$_{H_2}$ of $1.9 \cdot 10^6$. A bias-free semi-artificial water splitting H_2 evolution device was produced using the PVK|IO-TiO$_2$|H$_2$ase photocathode and a water oxidising BiVO$_4$ photoanode. In a single compartment 'leaf' configuration, the tandem PEC system was shown to be potential generating with an onset potential of -0.6 V and a solar-to-hydrogen efficiency of 1.1%. This work provides a new benchmark for photocathodes and tandem PEC devices employing earth-abundant molecular H_2 production catalysts. This system demonstrates the potential for bias-free fuel production and establishes perovskites as a suitable photoelectrode material for the integration of biocatalysts.

ASSOCIATED CONTENT

Supporting Information

The Supporting Information is available free of charge on the ACS Publications website at DOI:

Experimental procedures, photovoltaic parameters of perovskite cells, SEM of IO-TiO$_2$ electrode, 3D representation of the [NiFeSe] H$_2$ase enzyme, protein film voltammetry of Ti|IO-TiO$_2$|H$_2$ase electrode, photoelectrochemistry of the BiVO$_4$ photoanode, additional tandem device studies and performance comparison radar plots and tables of state-of-the-art photocathodes and tandem devices.

AUTHOR INFORMATION

Corresponding Author

*reisner@ch.cam.ac.uk

Author Contributions

E.E.M., V.A. and E.R. designed the project. E.E.M synthesized and characterized the IO-TiO$_2$ material, encapsulated the devices and carried out the electrochemistry and photoelectrochemistry. V.A. prepared and characterized the perovskite solar cells and the BiVO$_4$ photoanodes. S.Z. and I.A.C.P. expressed, purified and characterized the DvH [NiFeSe] hydrogenase. E.E.M., V.A. and E.R. analyzed the data. E.E.M. and E.R. wrote the manuscript with contributions and discussions from all authors. E.R. supervised the research work.

Notes
The authors declare no competing financial interests.

REFERENCES

1.   Coyle, E. D.; Simmons, R. A., *Understanding the Global Energy Crisis*. Purdue University Press: Lafayette, March 2014.

2.   Nayak, P. K.; Mahesh, S.; Snaith, H. J.; Cahen, D., Photovoltaic solar cell technologies: analysing the state of the art. *Nat. Rev. Mater.* **2019,** *4*, 269.

3.   Tachibana, Y.; Vayssieres, L.; Durrant, J. R., Artificial photosynthesis for solar water-splitting. *Nat. Photon.* **2012,** *6*, 511-518.

4.   Dalle, K. E.; Warnan, J.; Leung, J. J.; Reuillard, B.; Karmel, I. S.; Reisner, E., Electro- and Solar-driven Fuel Synthesis with First Row Transition Metal Complexes. *Chem. Rev.* **2019,** *119* (4), 2752-2875.

5.   Jia, J.; Seitz, L. C.; Benck, J. D.; Huo, Y.; Chen, Y.; Ng, J. W. D.; Bilir, T.; Harris, J. S.; Jaramillo, T. F., Solar water splitting by photovoltaic-electrolysis with a solar-to-hydrogen efficiency over 30%. *Nat. Commun.* **2016,** *7*, 13237.

6.   Hisatomi, T.; Kubota, J.; Domen, K., Recent advances in semiconductors for photocatalytic and photoelectrochemical water splitting. *Chem. Soc. Rev.* **2014,** *43* (22), 7520-7535.

7.   National Renewable Energy Laboratory. https://www.nrel.gov/pv/assets/pdfs/best-research-cell-efficiencies.20191106.pdf (accessed November 2019).

8.   Green, M. A.; Ho-Baillie, A.; Snaith, H. J., The emergence of perovskite solar cells. *Nat. Photonics* **2014,** *8*, 506-514.

9.   Jiang, Q.; Chu, Z.; Wang, P.; Yang, X.; Liu, H.; Wang, Y.; Yin, Z.; Wu, J.; Zhang, X.; You, J., Planar-Structure Perovskite Solar Cells with Efficiency beyond 21%. *Adv. Mater.* **2017,** *29*, 1703852.

10.   Kim, H.-S.; Hagfeldt, A.; Park, N.-G., Morphological and compositional progress in halide perovskite solar cells. *Chem. Commun.* **2019,** *55*, 1192-1200.

11.   Da, P.; Cha, M.; Sun, L.; Wu, Y.; Wang, Z. S.; Zheng, G., High-performance perovskite photoanode enabled by Ni passivation and catalysis. *Nano. Lett.* **2015,** *15* (5), 3452-3457.

12.   Correa-Baena, J.-P.; Abate, A.; Saliba, M.; Tress, W.; Jacobsson, T. J.; Grätzel, M.; Hagfeldt, A., The rapid evolution of highly efficient perovskite solar cells. *Energy Environ. Sci.* **2017,** *10*, 710-727.

13.   Crespo-Quesada, M.; Pazos-Outón, L. M.; Warnan, J.; Kuehnel, M. F.; Friend, R. H.; Reisner, E., Metal-encapsulated organolead halide perovskite photocathode for solar-driven hydrogen evolution in water. *Nat. Commun.* **2016,** *7*, 12555.

14.   Zhang, H.; Yang, Z.; Yu, W.; Wang, H.; Ma, W.; Zong, X.; Li, C., A Sandwich-Like Organolead Halide Perovskite Photocathode for Efficient and Durable Photoelectrochemical Hydrogen Evolution in Water. *Adv. Energy Mater.* **2018,** *8*, 1800795.

15.   Andrei, V.; Hoye, R. L. Z.; Crespo-Quesada, M.; Bajada, M.; Ahmad, S.; Volder, M. D.; Friend, R.; Reisner, E., Scalable Triple Cation Mixed Halide Perovskite–BiVO4 Tandems for Bias-Free Water Splitting. *Adv. Energy Mater.* **2018,** *8*, 1801403.

16.   Poli, I.; Hintermair, U.; Regue, M.; Kumar, S.; Sackville, E. V.; Baker, J.; Watson, T. M.; Eslava, S.; Cameron, P. J., Graphite-protected CsPbBr3 perovskite photoanodes functionalised with water oxidation catalyst for oxygen evolution in water. *Nat. Commun.* **2019,** *10*, 2097.

17.   Crespo-Quesada, M.; Reisner, E., Emerging approaches to stabilise photocorrodible electrodes and catalysts for solar fuel applications. *Energy Environ. Sci.* **2017,** *10*, 1116-1127.

18.   Kornienko, N.; Zhang, J. Z.; Sakimoto, K. K.; Yang, P.; Reisner, E., Interfacing nature's catalytic machinery with synthetic materials for semi-artificial photosynthesis. *Nat. Nanotech.* **2018,** *13*, 890-899.

19.   Evans, R. M.; Siritanaratkul, B.; Megarity, C. F.; Pandey, K.; Esterle, T. F.; Badiani, S.; Armstrong, F. A., The value of enzymes in solar fuels research – efficient electrocatalysts through evolution. *Chem. Soc. Rev.* **2019,** *48*, 2039-2052.

20.   Kim, J. H.; Na, D. H.; Park, C. B., Nanobiocatalytic assemblies for artificial photosynthesis. *Curr. Opin. Biotechnol.* **2014,** *28*, 1-9.

21.   Lee, S. H.; Choi, D. S.; Kuk, S. K.; Park, C. B., Photobiocatalysis: Activating Redox Enzymes by Direct or Indirect Transfer of Photoinduced Electrons. *Angew. Chem. Int. Ed.* **2018,** *57* (27), 7958-7985.

22.   Tran, P. D.; Barber, J., Proton reduction to hydrogen in biological and chemical systems. *Phys. Chem. Chem. Phys.* **2012,** *14*, 13772-13784.

23.   Lubitz, W.; Ogata, H.; Rüdiger, O.; Reijerse, E., Hydrogenases. *Chem. Rev.* **2014,** *114*, 4081-4148.

24.   Jones, A. K.; Sillery, E.; Albracht, S. P. J.; Armstrong, F. A., Direct comparison of the electrocatalytic oxidation of hydrogen by an enzyme and a platinum catalyst. *Chem. Commun.* **2002,** 866-867.

25.   Nam, D. H.; Zhang, J. Z.; Andrei, V.; Kornienko, N.; Heidary, N.; Wagner, A.; Nakanishi, K.; Sokol, K. P.; Slater, B.; Zebger, I.; Hofmann, S.; Fontecilla-Camps, J. C.; Park, C. B.; Reisner, E., Solar Water Splitting with a Hydrogenase Integrated in Photoelectrochemical Tandem Cells. *Angew. Chem. Int. Ed.* **2018,** *57*, 10595-10599.

26.   Zhao, Y.; Anderson, N. C.; Ratzloff, M. W.; Mulder, D. W.; Zhu, K.; Turner, J. A.; Neale, N. R.; King, P. W.; Branz, H. M., Proton Reduction Using a Hydrogenase-Modified Nanoporous Black Silicon Photoelectrode. *ACS Appl. Mater. Interfaces* **2016,** *8* (23), 14481–14487.

27.   Tiana, L.; Németh, B.; Berggren, G.; Tian, H., Hydrogen evolution by a photoelectrochemical cell based on a Cu2O-ZnO-[FeFe] hydrogenase electrode. *J. Photochem. Photobiol. A: Chem.* **2018,** *366*, 27-33.

28.   Leung, J. J.; Warnan, J.; Nam, D. H.; Zhang, J. Z.; Willkomm, J.; Reisner, E., Photoelectrocatalytic H2 evolution in water with molecular catalysts immobilised on p-Si *via* a stabilising mesoporous TiO2 interlayer. *Chem. Sci.* **2017,** *8*, 5172-5180.

29.   Lee, C. Y.; Park, H. S.; Fontecilla-Camps, J. C.; Reisner, E., Photoelectrochemical H2 Evolution with a Hydrogenase Immobilized on a TiO2-Protected Silicon Electrode. *Angew. Chem. Int. Ed.* **2016,** *55* (20), 5971-5974.

30.   Mersch, D.; Lee, C.-Y.; Zhang, J. Z.; Brinkert, K.; Fontecilla-Camps, J. C.; Rutherford, A. W.; Reisner, E., Wiring of Photosystem II to Hydrogenase for Photoelectrochemical Water Splitting. *J. Am. Chem. Soc.* **2015,** *137*, 8541–8549.

31.   Sokol, K. P.; Robinson, W. E.; Warnan, J.; Kornienko, N.; Nowaczyk, M. M.; Ruff, A.; Zhang, J. Z.; Reisner, E., Bias-free photoelectrochemical water splitting with photosystem II on a dye-sensitized photoanode wired to hydrogenase. *Nat. Energy* **2018,** *3*, 944-951.

32.   Miller, M.; Robinson, W. E.; Oliveira, A. R.; Heidary, N.; Kornienko, N.; Warnan, J.; Pereira, I. A. C.; Reisner, E., Interfacing Formate Dehydrogenase with Metal Oxides for the Reversible Electrocatalysis and Solar-Driven Reduction of Carbon Dioxide. *Angew. Chem. Int. Ed.* **2019,** *131* (14), 4649-4653.

33.   Wombwell, C.; Caputo, C. A.; Reisner, E., [NiFeSe]-Hydrogenase Chemistry. *Acc. Chem. Res.* **2015,** *48*, 2858–2865.

34.   Zacarias, S.; Véle, M.; Pita, M.; Lacey, A. L. D.; Matias, P. M.; Pereira, I. A. C., Characterization of the [NiFeSe] hydrogenase from *Desulfovibrio vulgaris* Hildenborough. *Meth. Enzymol.* **2018,** *613*, 169-201.

35.   Gutierrez-Sanchez, C.; Rudiger, O.; Fernandez, V. M.; De Lacey, A. L.; Marques, M.; Pereira, I. A., Interaction of the active site of the Ni-Fe-Se hydrogenase from *Desulfovibrio vulgaris* Hildenborough with carbon monoxide and oxygen inhibitors. *J. Biol. Inorg. Chem.* **2010,** *15* (8), 1285-1292.

36.   Valente, F. M. A.; Oliveira, A. S. F.; Gnadt, N.; Pacheco, I.; Coelho, A. V.; Xavier, A. V.; Teixeira, M.; Soares, C. M.; Pereira, I. A. C., Hydrogenases in *Desulfovibrio vulgaris* Hildenborough: structural and physiologic characterisation of the membrane-bound [NiFeSe] hydrogenase. *J. Biol. Inorg. Chem.* **2005,** *10* (6), 667-682.

37.   Marques, M. C.; Tapia, C.; Gutiérrez-Sanz, O.; Ramos, A. R.; Keller, K. L.; Wall, J. D.; Lacey, A. L. D.; Matias, P. M.; Pereira, I. A. C., The direct role of selenocysteine in [NiFeSe] hydrogenase maturation and catalysis. *Nat. Chem. Biol.* **2017,** *13*, 544-550.

38.   Marques, M. C.; Coelho, R.; De Lacey, A. L.; Pereira, I. A.; Matias, P. M., The three-dimensional structure of [NiFeSe] hydrogenase from *Desulfovibrio vulgaris* Hildenborough: a hydrogenase without a bridging ligand in the active site in its oxidised, "as-isolated" state. *J. Mol. Biol.* **2010,** *396* (4), 893-907.

39.   De Lacey, A. L.; Gutierrez-Sanchez, C.; Fernandez, V. M.; Pacheco, I.; Pereira, I. A., FTIR spectroelectrochemical characterization of the Ni-Fe-Se hydrogenase from *Desulfovibrio vulgaris* Hildenborough. *J. Biol. Inorg. Chem.* **2008,** *13* (8), 1315-1320.

40.   Parkin, A.; Goldet, G.; Cavazza, C.; Fontecilla-Camps, J. C.; Armstrong, F. A., The Difference a Se Makes? Oxygen-Tolerant Hydrogen Production by the [NiFeSe]-Hydrogenase from *Desulfomicrobium baculatum. J. Am. Chem. Soc.* **2008,** *130* (40), 13410-13416.

41.   Leader, A.; Mandler, D.; Reches, M., The role of hydrophobic, aromatic and electrostatic interactions between amino acid residues and a titanium dioxide surface. *Phys. Chem. Chem. Phys.* **2018,** *20*, 29811-29816.

42.   Li, F.; Fan, K.; Xu, B.; Gabrielsson, E.; Daniel, Q.; Li, L.; Sun, L., Organic Dye-Sensitized Tandem Photoelectrochemical Cell for Light Driven Total Water Splitting. *J. Am. Chem. Soc.* **2015,** *137*, 9153-9159.

43. Zhang, K.; Ma, M.; Li, P.; Wang, D. H.; Park, J. H., Water Splitting Progress in Tandem Devices: Moving Photolysis beyond Electrolysis. *Adv. Energy Mater.* **2016,** *6* (15), 1600602.

44. Lai, Y. H.; Palm, D. W.; Reisner, E., Multifunctional Coatings from Scalable Single Source Precursor Chemistry in Tandem Photoelectrochemical Water Splitting. *Adv. Energy Mater.* **2015,** *5* (24), 1501668.

45. Khusnutdinova, D.; Beiler, A. M.; Wadsworth, B. L.; Jacob, S. I.; Moore, G. F., Metalloporphyrin-modified semiconductors for solar fuel production. *Chem. Sci.* **2017,** *8*, 253-259.

46. Beiler, A. M.; Khusnutdinova, D.; Wadsworth, B. L.; Moore, G. F., Cobalt Porphyrin–Polypyridyl Surface Coatings for

Photoelectrosynthetic Hydrogen Production. *Inorg. Chem.* **2017,** *56* (20), 12178-12185.

47. Windle, C.; Kumagai, H.; Higashi, M.; Brisse, R.; Bold, S.; Jousselme, B.; Chavarot-Kerlidou, M.; Maeda, K.; Abe, R.; Ishitani, O.; Artero, V., Earth-Abundant Molecular Z-Scheme Photoelectrochemical Cell for Overall Water-Splitting. *J. Am. Chem. Soc.* **2019,** *141* (24), 9593-9602.

48. Liu, C.; Gallagher, J. J.; Sakimoto, K. K.; Nichols, E. M.; Chang, C. J.; Chang, M. C. Y.; Yang, P., Nanowire–Bacteria Hybrids for Unassisted Solar Carbon Dioxide Fixation to Value-Added Chemicals. *Nano Lett.* **2015,** *15*, 3634-3639.

TOC Artwork

Hydrogenase-Perovskite||BiVO$_4$